

RoomPainter: View-Integrated Diffusion for Consistent Indoor Scene Texturing

Zhipeng Huang¹ Wangbo Yu^{1,2} Xinhua Cheng¹ ChengShu Zhao¹ Yunyang Ge¹ Mingyi Guo¹
Li Yuan^{1,2†} Yonghong Tian^{1,2†}

¹Peking University
²Pengcheng Laboratory



Figure 1. **RoomPainter** is capable of generating high-fidelity and consistent texture for a given room mesh.

Abstract

Indoor scene texture synthesis has garnered significant interest due to its important potential applications in virtual reality, digital media, and creative arts. Existing diffusion model-based researches either rely on per-view inpainting techniques, which are plagued by severe cross-view inconsistencies and conspicuous seams, or they resort to optimization-based approaches that entail substantial computational overhead. In this work, we present **RoomPainter**, a framework that seamlessly integrates efficiency and consistency to achieve high-fidelity texturing of indoor scenes. The core of **RoomPainter** features a zero-shot technique that effectively adapts a 2D diffusion model for 3D-consistent texture synthesis, along with a two-stage generation strategy that ensures both global and local consistency. Specifically, we introduce Attention-Guided Multi-View Integrated Sampling (**MVIS**) combined with a neighbor-integrated attention mechanism for zero-shot texture map generation. Using the **MVIS**, we firstly generate texture map for the entire room to ensure global consistency,

then adopt its variant, namely Attention-Guided Multi-View Integrated Repaint sampling (**MVRS**) to repaint individual instances within the room, thereby further enhancing local consistency. Experiments demonstrate that **RoomPainter** achieves superior performance for indoor scene texture synthesis in visual quality, global consistency, and generation efficiency.

1. Introduction

High-quality 3D content synthesis is in great demand, owing to its diverse applications across the entertainment industry, robotic simulation, and mixed-reality environments. With the advancement of text-to-image diffusion models [28, 30, 33, 34], large-scale indoor scene texture synthesis has made significant progress. Although existing indoor texture synthesis methods produce high-quality results, they face several significant challenges. Specifically, these methods can be categorized into two groups: inpainting-based methods [5, 32] and optimization-based methods [6, 24, 47]. On one hand, the inpainting-based methods utilize depth-to-image diffusion models [33, 51] to

[†]Corresponding author.

progressively generate textures for neighboring views, with the guidance of reference geometry and previously generated views. However, due to their per-view inpainting strategy, these approaches often lead to inconsistencies in texture style and semantics across non-adjacent views, and do not effectively address the loop-closure problem. On the other hand, optimization-based methods mitigate these inconsistencies by employing score distillation loss [29] or its variations [43] in global texture maps. However, the optimization process incurs significant time costs for indoor texture synthesis and faces training instability, which may introduce significant artifacts.

To address these challenges, we propose an efficient and high-fidelity indoor scene texturing framework, dubbed **RoomPainter**. The core of RoomPainter lies in a zero-shot technique that effectively adapts a 2D diffusion model for 3D-consistent texture synthesis, along with a two-stage generation strategy that ensures both global and local consistency. Specifically, we introduce Attention-Guided Multi-View Integrated Sampling (MVIS) combined with a related view-based attention mechanism for zero-shot texture map generation. Using the MVIS, we can generate a holistic texture map for the entire room, achieving better global consistency than per-view inpainting-based methods. Subsequently, to address the untextured areas raised by occlusions between objects while preserving the global consistency established in the first stage, we adopt a refine stage to decouple each instance in the room, then apply an Attention-Guided Multi-view Integrated Repaint Sampling (MVRS) technique at the instance scale to perform texture inpainting and refinement for each individual instance.

The main contributions of our work are summarized below:

- We propose **RoomPainter**, an effective framework for indoor scene texture synthesis that excels in producing consistent, high-quality textures with remarkable time efficiency.
- We introduce Multi-View Integrated Sampling (MVIS), a zero-shot technique that leverages view-weighted texture rectification and related view-based attention to generate global consistent texture map using 2D diffusion model.
- We further present Multi-view Integrated Repaint Sampling (MVRS), which simultaneously refines the textured areas and inpaints the occlusion areas based on their context, thereby facilitates fine-detailed texture synthesis with local consistency.
- We conduct extensive experiments and compare our method with strong baselines. The results demonstrate that our method not only achieves superior performance in visual quality for indoor texture synthesis but also excels in generation efficiency.

2. Related Works

2.1. 3D Generation with Diffusion Model

With the rapid advancements in image [26, 28, 33, 34, 51] and video generation models [3, 44] in recent years, the field of 3D generation has experienced significant progress. Various methods now generate objects [8, 29, 41–43, 48] or scenes [10, 23, 49, 52] based on textual descriptions via leveraging SDS Loss and its variants [29, 43] to optimize implicit representation such as NeRF [25] and 3D Gaussian Splatting [19]. In the realm of scene generation, some approaches utilize text-guided inpainting models and depth prediction models, which incrementally construct scenes via a warping process [9, 11, 17, 27, 50]. Other methods focus on fine-tuning image generation models using 3D data, allowing them to generate multi-view consistent images or panorama for 3D tasks with the guidance of semantic images or depth maps. Moreover, some methods predict depth from a given image to initialize 3D Gaussian Splatting, followed by further optimization of the 3D Gaussian Splatting using video generation models.

2.2. 3D Object Texturing

The goal of 3D object texturing methods is to create high-quality texture for the given 3D object that align with user-provided textual descriptions. Early methods, such as [5, 32, 39], utilized depth-aware Diffusion Models [26, 33, 51] to iteratively apply inpainting for each viewpoint. At each step, the texture is generated based on the texture from the previous viewpoint, gradually rotating the object to produce a complete texture. While these methods can generate textures in a relatively short time, they fail to address issues such as loop-closure and visible seams. Other works, such as [7, 24, 47], leverage differentiable rendering combined with SDS [29] to texture the given object through optimization techniques. Additionally, approaches like [4, 13, 18, 21] use UV maps as intermediaries and apply different fusion methods to integrate multiple of view independent UV maps into a consistent UV map. During the Diffusion model sampling process, this consistent UV map is used to adjust the Diffusion model’s input, ensuring that the resulting texture is more consistent, with fewer visible seams and improved multi-view consistency.

2.3. 3D Indoor Scene Texturing

In the task of 3D indoor scene texture generation, the objective is to create textures for a given indoor scene based on a user-provided textual description, which presents challenges such as object occlusion and multi-view consistency. SceneTex [6] defines an implicit texture field and optimizes it using VSD [43]. By employing an optimization-based approach to refine the texture field, SceneTex naturally resolves the issue of multi-view consistency in 3D scene tex-

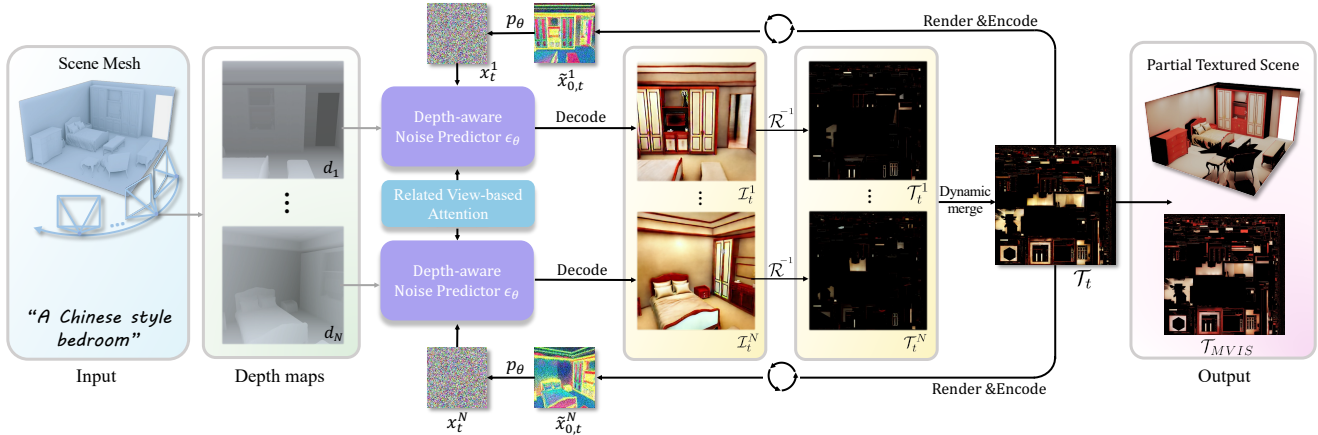


Figure 2. **Illustration of Multi-view Integrated Sampling** For N viewpoints in the room, guided by the corresponding depth maps, we use a Diffusion model to generate the denoised observation \mathcal{I}_t^n at timestep t . This observation is then projected into UV space to obtain the texture map for the respective viewpoint. The texture maps from multiple viewpoints are dynamically merged to produce the texture map for the current timestep, which subsequently guides the sampling process for the next timestep.

tures. Furthermore, SceneTex incorporates a cross-attention mechanism to transfer textures from visible regions to occluded areas. However, this process can result in blurriness in the occluded regions, and the optimization procedure itself is computationally intensive. When methods like Text2Tex and TEXTure [5, 32], typically used for object texture generation, are applied to scene texture generation, they can only enforce style consistency across multiple objects based on textual control. However, these methods do not ensure global style consistency for the entire scene. Alternatively, if the entire room is treated as a single object and methods such as TEXTure or Text2Tex are employed with the camera positioned at the center of the room, generating the scene texture by rotating the camera, global style consistency can be achieved. However, this approach still faces challenges such as occlusion and visible seams between regions.

Other approaches, such as [45], use panoramic images to generate a rough texture for the entire room. The camera position is then changed to generate textures for occluded regions. Subsequently, an MLP is employed to predict the textures of unseen areas based on the color and texture coordinates from the UV map. However, this method requires the scene to have an initial texture and relies on texture style transfer, meaning it cannot generate textures from scratch for a completely untextured scene.

3. Methods

Given a 3D indoor scene mesh \mathcal{M} , our objective is to efficiently generate textures that not only align with the provided textual descriptions but also maintain coherent semantics. Since our framework employs pretrained T2I Diffusion model to generate textures for the given indoor scene

mesh, we will start with an overview of the T2I Diffusion model and mesh rendering in Sec. 3.1. Following this, we introduce Multi-view Integrated Sampling (abbreviated as **MVIS**) in Sec. 3.2, which addresses the challenge of maintaining multi-view consistency while preserving high-frequency details in the diffusion model sampling process. Subsequently, In Sec. 3.3, we introduce a variant of **MVIS**, namely Multi-view Integrated Repaint Sampling (**MVRS**), to address the occlusion region and simultaneously refine existing textures. Finally, in Sec. 3.4, we introduce a Related View-based Attention mechanism used in the **MVIS** and **MVRS** processes to achieve more consistent image generation.

3.1. Preliminaries

Diffusion Model Sampling. Diffusion models [16, 38] are latent variable models that comprises a forward process $q(x_t|x_0)$ and a learned sampling process $p_\theta(x_{t-1}|x_t)$. Given an initial data point x_0 , its noisy counterpart at time t is denoted as x_t , and the forward process q can be expressed as:

$$x_t = \sqrt{\bar{\alpha}_t}x_0 + \sqrt{(1 - \bar{\alpha}_t)}\epsilon, \epsilon \sim N(0, I), \quad (1)$$

where $t \in [0, \infty)$ and the values of α_t are defined by a scheduler to controls the amount of noise added at time step t . Additionally, it has $\beta_t = 1 - \alpha_t$ and $\bar{\alpha}_t = \prod_{s=1}^t \alpha_s$. In the sampling process p_θ , with the DDPM sampler [16], the diffusion model progressively denoises an initial noise image $x_T \sim \mathcal{N}(0, I)$ to clean image. Specifically, at any intermediate time step t , the sampling process p_θ can be formed as:

$$x_{t-1} = \mu_{t-1} + \sigma_t\epsilon, \epsilon \sim N(0, I), \quad (2)$$

where the value of σ_t and μ_{t-1} is given by:

$$\mu_{t-1} = \frac{\sqrt{\bar{\alpha}_{t-1}}\beta_t}{1 - \bar{\alpha}_t}x_{0,t} + \frac{\sqrt{\bar{\alpha}_t}(1 - \bar{\alpha}_{t-1})}{1 - \bar{\alpha}_t}x_t, \quad (3)$$

$$\sigma_t = \frac{1 - \bar{\alpha}_{t-1}}{1 - \bar{\alpha}_t}\beta_t, \quad (4)$$

and the estimation of the original image $x_{0,t}$ at time step t is calculated as:

$$x_{0,t} = \frac{x_t - \sqrt{1 - \bar{\alpha}_t}\epsilon_\theta(x_t, t)}{\sqrt{\bar{\alpha}_t}}, \quad (5)$$

where $\epsilon_\theta(x_t, t)$ is the estimated noise. As t decreases from T to 0, the sampling process p_θ ultimately samples a clean data point x_0 . Moreover, this process can be generalized for learning a marginal distribution using an additional input condition. That leads depth-aware text-to-image diffusion models [1, 51], where the output of the model $\epsilon_\theta(x_t, y, d, t)$ is conditioned on a text prompt y and a depth map d .

In this paper, we utilize Stable Diffusion [28] as our base model. It performs denoising in the latent space and employs an autoencoder $\mathcal{D}(\mathcal{E}(\cdot))$ for the conversion between image and latent representations. Therefore, x_0 generated by its diffusion process will be decoded to the image $\mathcal{D}(x_0)$ through its decoder.

Mesh Rendering. Given a mesh \mathcal{M} , a texture map \mathcal{T} and a viewpoint C , the rendering function \mathcal{R} can be employed to produce the rendered image as $I = \mathcal{R}(\mathcal{T}, \mathcal{M}, C)$. Conversely, the inverse rendering function: \mathcal{R}^{-1} can reconstruct the texture map from the image, yielding $\mathcal{T}' = \mathcal{R}^{-1}(I, \mathcal{M}, C)$.

3.2. Multi-view Integrated Sampling

Different from object-level multi-view diffusion models [20, 36, 37], diffusion models that capable of ensuring multi-view consistency in scene level image generation [40] are extremely limited. To address this challenge, we propose Multi-view Integrated Sampling (MVIS), grounded with a Related View-based Attention technique, to adapt a standard T2I model to generate view-consistent images in a training-free manner. Based on MVIS, we first implement a global texturing stage to generate consistent textures for the scene mesh.

As shown in Fig. 2, given a set of predefined cameras $\{C\} = C^n, n = 1, \dots, N$, we first render their corresponding depth maps d_n and similarity masks S_n , where each pixel in the similarity mask represents the inverted normalized value of the cosine similarity between the normal vectors of the visible faces and the viewing direction, with values ranging from $[0, 1]$ [5, 13, 32]. Based on the similarity masks, we construct the texture weighting maps W_n for each camera, defined as $W_n = \mathcal{R}^{-1}(S_n, \mathcal{M}, C^n)$, which are then used to dynamically merge per-view texture maps.

Algorithm 1 Multi-view Integrated Sampling

Input: mesh \mathcal{M} , text y , cameras $\{C^1, \dots, C^N\}$

Parameters: DDPM noise schedule $\{\sigma_t\}_{t=T}^0$

Initialization: $\{x_T^n\}_{n=1}^N \sim \{\mathcal{N}(0, I)\}$

for $t \in \{T \dots 0\}$ **do**

for $n \in \{1 \dots N\}$ **do**

$\epsilon_t^n \leftarrow \epsilon_\theta(x_t^n, y, d_n, t)$

$x_{0,t}^n \leftarrow \frac{x_t^n - \sqrt{1 - \bar{\alpha}_t}\epsilon_t^n}{\sqrt{\bar{\alpha}_t}}$

$\mathcal{I}_t^n \leftarrow \mathcal{D}(x_{0,t}^n)$

$\mathcal{T}_t^n \leftarrow \mathcal{R}^{-1}(\mathcal{I}_t^n, \mathcal{M}, C^n)$

end for

$\mathcal{T}_t = \text{dynamic_merge}(\{\mathcal{T}_t^n\}_{n=1}^N)$

if $t > 0$ **then**

for $n \in \{1 \dots N\}$ **do**

$\epsilon^n \sim \mathcal{N}(0, I)$

$\tilde{x}_{0,t}^n \leftarrow \mathcal{E}(M^n \odot \mathcal{R}(\mathcal{T}_t, \mathcal{M}, C_n) + (1 - M^n) \odot \mathcal{I}_t^n)$

$\mu_{t-1}^n \leftarrow \frac{\sqrt{\bar{\alpha}_{t-1}}\beta_t}{1 - \bar{\alpha}_t}\tilde{x}_{0,t}^n + \frac{\sqrt{\bar{\alpha}_t}(1 - \bar{\alpha}_{t-1})}{1 - \bar{\alpha}_t}x_t^n$

$x_{t-1}^n \leftarrow \mu_{t-1}^n + \sigma_t\epsilon^n$

end for

end if

end for

$\mathcal{T}_{MVIS} = \mathcal{T}_0$

return Texture map \mathcal{T}_{MVIS}

As shown in Algorithm. 1, in the sampling process, we firstly sample $\{x_T^n\}_{n=1}^N \sim \{\mathcal{N}(0, I)\}$ for the N camera views. Subsequently, in each denoising step t , we decode all N estimated $x_{0,t}^n$ into \mathcal{I}_t^n and back project them into individual per-view texture map \mathcal{T}_t^n . We then merge these per-view texture maps to form a global texture map \mathcal{T}_t using dynamic merge [2, 21], which can be formulated as:

$$\mathcal{T}_t = \frac{\sum_{n=1}^N (W_n^{exp(t)} \cdot \mathcal{T}_t^n)}{\sum_{n=1}^N W_n + \gamma}. \quad (6)$$

Here, $exp(t)$ is used to dynamically regulate variations in consistency during the sampling process at timestep t . As t decreases, $exp(t)$ increases linearly, leading to a sharper merged texture. With the merged texture map, we again render per view images from \mathcal{T}_t , using foreground mask M^n for viewpoint C^n , and encode them into latent space to obtain $\tilde{x}_{0,t}$, which is then used to replace the previous obtained less $x_{0,t}^n$ in Eq. 3 for consistent view generation. After repeating these denoising steps, we are able to generate a consistent texture map, denote as \mathcal{T}_{MVIS} .

3.3. Multi-view Integrated Repaint Sampling

Although the texture map \mathcal{T}_{MVIS} maintains stylistic and consistent throughout the room, there are still areas that remain untextured due to occlusions. To address this prob-

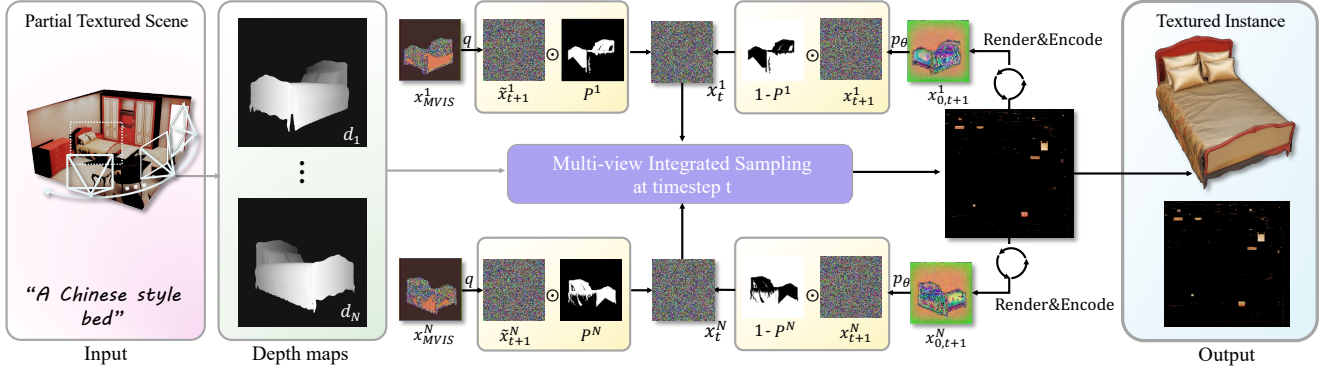


Figure 3. **Illustration of Multi-view Integrated Repaint Sampling (MVRS)** Due to occlusion between instances, some areas remain untextured after the first stage of texture generation. To address this issue, we perform texture generation for each instance in the room, conditioned on the painted areas. For the N different viewpoints of each instance, guided by the corresponding depth maps, at sampling step t of MVRS, we combine the painted areas: x_{MVIS} with the sampling results of MVIS at step $t + 1$: $x_{0,t+1}$ using a mask P . to form x_t , which serves as the input for the sampling process of the timestep t . Noise that corresponding to the current timestep was added before mask combine. Upon completing the MVRS sampling process, the textures for all instances in the room are fully generated.

lem, we adopt a refine stage to inpaint the occlusion areas and further enhance the texture fidelity, while preserving the global consistency established in the first stage.

Specifically, we decouple each instance in the room, resulting a total of K instances $\mathcal{M}_1, \dots, \mathcal{M}_K$. We then design a variant of **MVIS**, namely multi-view integrated repaint sampling (**MVRS**), to perform texture inpainting and refinement for each individual instance. As shown in Fig. 3, the core of **MVRS** lies in incorporating diffusion-based inpainting [22] into the **MVIS** process. For each individual instance, given N predefined camera views, we firstly render N images \mathcal{T}^n along with their inpainting masks P^n that indicates untextured region of them. Subsequently, for any time step t in the **MVIS** process, we encode \mathcal{T}^n into the latent space and add noise on it to produce a noisy latent \tilde{x}_t^n , followed by sampling x_t^n from **MVIS**, then combine them into a new latent using the inpainting mask P^n , finally passing it into the U-Net for the next denoising step. This process introduces information from the painted area into the **MVIS** process, effectively transferring the texture of the painted area to the regions with holes while ensuring consistency across multiple viewpoints. After iterating through all instances within the room, we obtain the final output scene texture \mathcal{T}_{MVRS} .

3.4. Related View-based Attention

In the **MVIS** and **MVRS** process, we employ a 2D Diffusion Model for zero-shot multi-view sampling. A key challenge in maintaining view consistency is sharing information across multiple images from different viewpoints. Inspired by [14], we modify the self-attention mechanism in the diffusion model to ensure that each view incorporates sampling information from related views during the

sampling process. During the sampling process, denote the queries, keys and values derived from the deep feature of the denoising U-Net for viewpoint n as Q_n , K_n , and V_n , respectively. For each viewpoint, assume that it has a total of R associated viewpoints (view that has overlap). Subsequently, the Related View-based Attention for viewpoint n is computed as:

$$\text{softmax} \left(\frac{Q_n \tilde{K}_n^T}{\sqrt{d}} \tilde{V}_n \right), \quad (7)$$

where $\tilde{K}_n = \begin{bmatrix} K_1 \\ K_2 \\ \vdots \\ K_R \end{bmatrix}$ and $\tilde{V}_n = \begin{bmatrix} V_1 \\ V_2 \\ \vdots \\ V_R \end{bmatrix}$. In the first room-

scale texturing stage, we consider the related viewpoints R for view n as its adjacent views, *i.e.*, its left and right view. When sampling at instance scale, we define the related views as all the N predefined camera view.

4. Experiments

In this section, we first describe the general implementation of the baseline methods used for comparison. Next, we provide an overview of the implementation details of our proposed method. Finally, we present our quantitative experiments, qualitative results, and ablation studies.

4.1. Baseline Implementation Details

- **Text2Tex-H** [5]: This variant of Text2Tex is implemented using a holistic text prompt provided by user and treats the entire room as a cohesive entity. The camera is positioned at the center of the room, with a field of view of



Figure 4. **Qualitative comparisons.** Text2Tex-H [5] suffers from occlusion and visible seams. Text2Tex-C [5] struggles to maintain style consistency across all instances. SceneTex [6] produces unrealistic textures and results in blurry regions. In contrast, our method generates high-quality textures while preserving overall style consistency across instances in the scene. Ceilings and back-facing walls are excluded for improved visualizations.

60°, and the elevation angle is set to 0°, and azimuth angles uniformly sampled from the range [0°, 360°], which results in a total of twelve perspectives.

- Text2Tex-C [5]: For comparative purposes, we employ the original configuration of Text2Tex, wherein each room instance, including the interior walls and furniture, is textured using an instance-specific text prompt. And for interior walls texturing, we utilize the text prompt such as: "A Chinese style living room, no furniture" and sampled 12 perspectives same as Text2Tex-H. All the textured instances are subsequently combined, forming the output

textured room.

- SceneTex [6]: We compare against SceneTex using its original setup, while employing the same holistic prompt as utilized in our approach.

4.2. Implementation Details

In this experiment, we used the SDXL model [28] as the text-to-image (T2I) generator and incorporated depth information through ControlNet [1, 51]. For the text prompt, we implemented view-specific prompt combining the holistic

“A Cream style master bedroom”

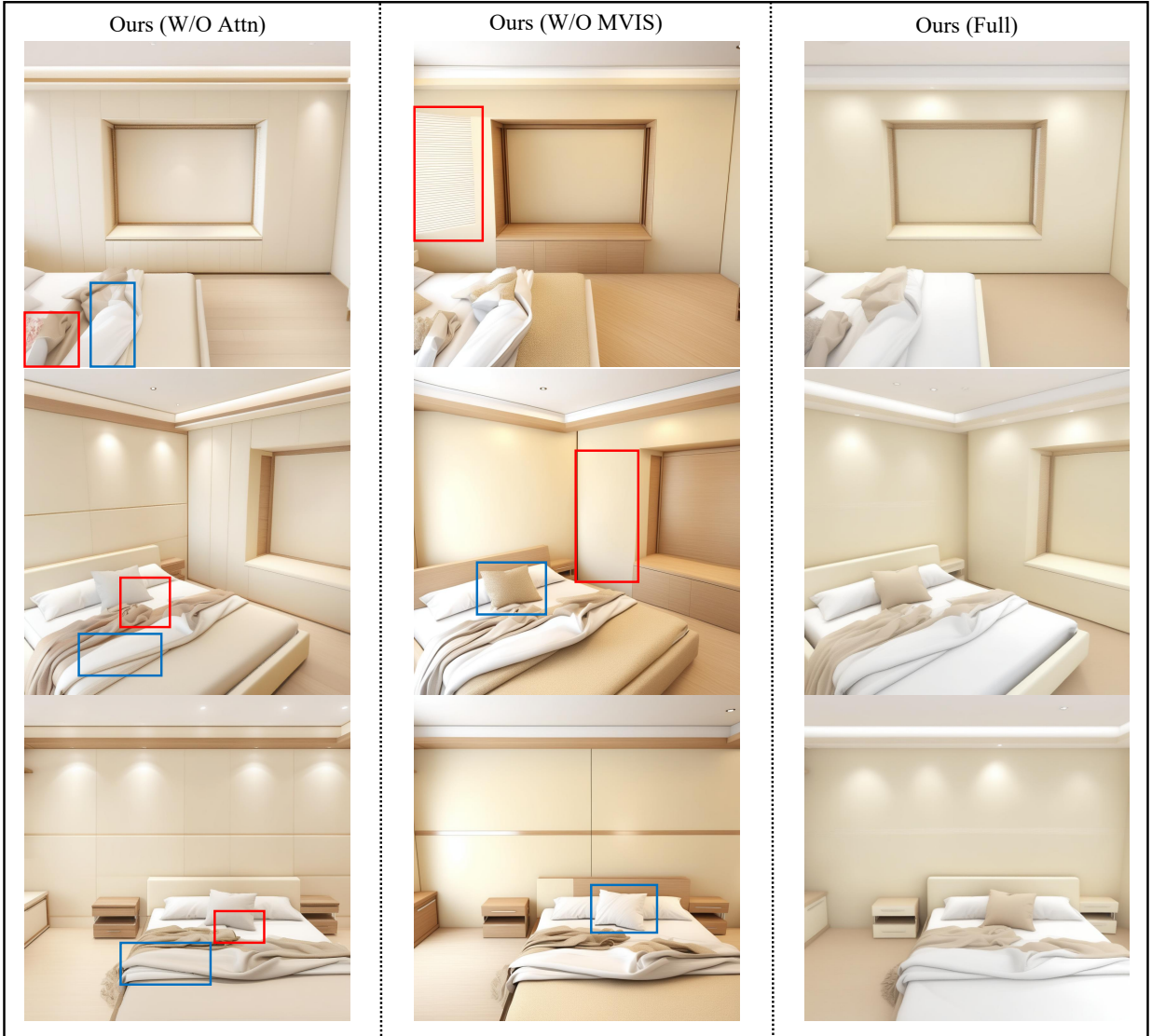


Figure 5. **Ablation studies on the multiview-consistency module.** Synthesizing texture without the Related View-based attention leads to inconsistencies across views, as shown in the leftmost column. When synthesizing texture without MVIS, noticeable inconsistencies appear across different viewpoints (middle column). In contrast, our full method samples multi-view images with significantly stronger consistency. The areas of major inconsistency in the images are highlighted with red and blue boxes. In the same column, boxes of the same color indicate that they are close to each other in 3D space. Zoom in for the best view.

prompt with the names of the types of objects present within the field of view. For sampling, we applied the DDPM [16] as the sampler, setting the sampling steps to 50. We used PyTorch3D [31] for rendering and texture projection. Additionally, UV atlas generation for the mesh was handled with Xatlas [46]. All experiments were performed on an NVIDIA RTX A6000 GPU. Further implementation details are available in the supplementary materials.

4.3. Quantitative Analysis

Our quantitative experiment were conducted across 10 scenes including 5 bedroom and 5 living room from the 3D-FRONT dataset [12], using five different text styles totally. To evaluate the generated texture, we calculated both the CLIP Score (CLIP) [15], which assesses the alignment between generated texture and the textual description, and the CLIP Aesthetic Score (AS) [35], which measures texture quality. We also compared the average processing time of each texture generation method in minutes. The results are

Method	Generation Time(mins) ↓	CLIP ↑	AS ↑
Text2Tex-H [5]	8.50	21.58	4.34
Text2Tex-C [5]	70.75	21.93	4.85
SceneTex [6]	2614.50	21.87	4.75
(Ours) Full	46.00	23.47	5.03
(Ours) w/o Attn	-	23.32	5.01
(Ours) w/o MVIS	-	23.27	5.01
(Ours) w/o MVRS	-	22.39	4.40

Table 1. **Quantitative comparisons.** We report the Generation time and 2D metrics result for quantitative comparisons. The generation time is shown in the format minutes. The 2D metrics includes: CLIP Score (CLIP) [15], Aesthetic Score(AS) [35]. We show that our method produces high quality textures efficiently.

summarized in Table.1. We render 10 images from novel views for each room to calculate the average of CLIP and AS. Due to the presence of numerous distinct objects within the room, the methods in the baselines do not adjust the text prompts for texture generation based on the variation of objects from different viewpoints. Therefore, we employ a holistic prompt to compute the CLIP score. Since our evaluation metric involves image sampling from new viewpoints, Text2Tex-H, which fails to address the occlusion problem, generates textures containing large occluded regions, resulting in the lowest performance in terms of the metric. However, due to the limited number of sampled viewpoints, it exhibits the fastest generation speed. We configure SceneTex according to its original setup, sampling from a sphere centered at the room’s center. As a result, regions not observed by SceneTex often exhibit blurriness. Meanwhile, in addition to optimizing the texture field using VSD, SceneTex also requires training LoRA, which results in the longest processing time. Text2Tex-C employs an instance-specific approach for texture generation, utilizing different prompts for each object, which results in higher performance metrics. Additionally, it incorporates view-point selection and texture optimization processes, leading to a longer computation time.

4.4. Qualitative Analysis

We provide a visual comparison in fig.4. Specifically, Text2Tex-H [5] shows that simply applying object texture generation method to indoor scene texturing task cannot resolve the occlusion problem (see the large black areas in the first column of fig.4) and contain obvious seams. Text2Tex-C [5] texturing the room completely but suffering from obvious seams and global style consistency across objects. Although SceneTex introduces the use of cross-attention to generate textures for occluded regions, noticeable blurriness still persists in these areas. Furthermore, due to its optimization-based approach, SceneTex often produces un-

realistic textures. In contrast, our method generates globally consistent textures with a unified style in the first stage. In the second stage, through per-instance inpainting and refinement, we successfully maintain global style consistency while addressing issues of occlusion and unrealistic textures.

4.5. Ablation Studies

Effectiveness of the MVIS. We employ a two-stage approach to generate textures for the room. In the first stage, we introduce MVIS to enhance the global consistency of the textures. Qualitative results from this stage are shown in second column of the Fig. 5. The figures demonstrate that without MVIS, texture consistency across multiple viewpoints can be significantly impact. We further conduct quantitative ablation on dataset adopted in previous experiments. Results are shown in the seventh row of Tab. 1. The quantitative experimental results clearly demonstrate that MVIS improves the quality of the generated textures. **Effectiveness of the Related View-based Attention.** We incorporate the Related View-based Attention module in both stages of texture generation to enhance consistency. Both qualitative(the first column of Fig. 5) and quantitative experiments(the fifth row of the Tab. 1) demonstrate that using only MVIS or MVRS is insufficient to generate consistent and high-quality textures. The Related View-based Attention module effectively enhances consistency while ensuring the quality of the generated textures. **Effectiveness of the MVRS.** In the second stage of texture generation, we use MVRS to generate textures for the occluded regions of each instance, while also refining the textures generated in the first stage. Quantitative experimental results (seventh row in Tab. 1) show that without MVRS, the quality of the textures significantly deteriorates. This is because, without MVRS, the textures generated in the first stage suffer from low-quality results due to occlusion. We will provide additional qualitative materials demonstrating the effectiveness of MVRS in the supplementary materials.

5. Conclusion

We propose an indoor scene texturing framework named RoomPainter that generates high-quality textures with multi-view consistency and time efficiency. By leveraging the carefully designed modules including view-weighted texture rectification and related view-based attention, proposed view-integrated diffusion preserves the cross-view consistency during the diffusion process. Qualitative and quantitative results demonstrate the effectiveness of RoomPainter in indoor scene texturing, especially in global consistency and generation efficiency.

References

- [1] xinsir/controlnet-depth-sdxl-1.0. <https://huggingface.co/xinsir/controlnet-depth-sdxl-1.0>, 2023. 4, 6
- [2] Raphael Bensadoun, Yanir Kleiman, Idan Azuri, Omri Harosh, Andrea Vedaldi, Natalia Neverova, and Oran Gafni. Meta 3d texturegen: Fast and consistent texture generation for 3d objects. *arXiv preprint arXiv:2407.02430*, 2024. 4
- [3] Andreas Blattmann, Tim Dockhorn, Sumith Kulal, Daniel Mendelevitch, Maciej Kilian, Dominik Lorenz, Yam Levi, Zion English, Vikram Voleti, Adam Letts, et al. Stable video diffusion: Scaling latent video diffusion models to large datasets. *arXiv preprint arXiv:2311.15127*, 2023. 2
- [4] Tianshi Cao, Karsten Kreis, Sanja Fidler, Nicholas Sharp, and Kangxue Yin. Textfusion: Synthesizing 3d textures with text-guided image diffusion models. In *Proceedings of the IEEE/CVF International Conference on Computer Vision*, pages 4169–4181, 2023. 2
- [5] Dave Zhenyu Chen, Yawar Siddiqui, Hsin-Ying Lee, Sergey Tulyakov, and Matthias Nießner. Text2tex: Text-driven texture synthesis via diffusion models. In *Proceedings of the IEEE/CVF International Conference on Computer Vision*, pages 18558–18568, 2023. 1, 2, 3, 4, 5, 6, 8
- [6] Dave Zhenyu Chen, Haoxuan Li, Hsin-Ying Lee, Sergey Tulyakov, and Matthias Nießner. Scenetex: High-quality texture synthesis for indoor scenes via diffusion priors. In *Proceedings of the IEEE/CVF Conference on Computer Vision and Pattern Recognition*, pages 21081–21091, 2024. 1, 2, 6, 8
- [7] Rui Chen, Yongwei Chen, Ningxin Jiao, and Kui Jia. Fantasia3d: Disentangling geometry and appearance for high-quality text-to-3d content creation. In *Proceedings of the IEEE/CVF international conference on computer vision*, pages 22246–22256, 2023. 2
- [8] Xinhua Cheng, Tianyu Yang, Jianan Wang, Yu Li, Lei Zhang, Jian Zhang, and Li Yuan. Progressive3d: Progressively local editing for text-to-3d content creation with complex semantic prompts. *arXiv preprint arXiv:2310.11784*, 2023. 2
- [9] Jaeyoung Chung, Suyoung Lee, Hyeongjin Nam, Jaerin Lee, and Kyoung Mu Lee. Luciddreamer: Domain-free generation of 3d gaussian splatting scenes. *arXiv preprint arXiv:2311.13384*, 2023. 2
- [10] Dana Cohen-Bar, Elad Richardson, Gal Metzger, Raja Giryes, and Daniel Cohen-Or. Set-the-scene: Global-local training for generating controllable nerf scenes. In *Proceedings of the IEEE/CVF International Conference on Computer Vision*, pages 2920–2929, 2023. 2
- [11] Rafail Fridman, Amit Abecasis, Yoni Kasten, and Tali Dekel. Scenescape: Text-driven consistent scene generation. *Advances in Neural Information Processing Systems*, 36, 2024. 2
- [12] Huan Fu, Bowen Cai, Lin Gao, Ling-Xiao Zhang, Jiaming Wang, Cao Li, Qixun Zeng, Chengyue Sun, Rongfei Jia, Bin-qiang Zhao, et al. 3d-front: 3d furnished rooms with layouts and semantics. In *Proceedings of the IEEE/CVF International Conference on Computer Vision*, pages 10933–10942, 2021. 7
- [13] Chenjian Gao, Boyan Jiang, Xinghui Li, Yingpeng Zhang, and Qian Yu. Genesisstex: Adapting image denoising diffusion to texture space. In *Proceedings of the IEEE/CVF Conference on Computer Vision and Pattern Recognition*, pages 4620–4629, 2024. 2, 4
- [14] Amir Hertz, Andrey Voynov, Shlomi Fruchter, and Daniel Cohen-Or. Style aligned image generation via shared attention. In *Proceedings of the IEEE/CVF Conference on Computer Vision and Pattern Recognition*, pages 4775–4785, 2024. 5
- [15] Jack Hessel, Ari Holtzman, Maxwell Forbes, Ronan Le Bras, and Yejin Choi. Clipscore: A reference-free evaluation metric for image captioning. *arXiv preprint arXiv:2104.08718*, 2021. 7, 8
- [16] Jonathan Ho, Ajay Jain, and Pieter Abbeel. Denoising diffusion probabilistic models. *Advances in neural information processing systems*, 33:6840–6851, 2020. 3, 7
- [17] Lukas Höllein, Ang Cao, Andrew Owens, Justin Johnson, and Matthias Nießner. Text2room: Extracting textured 3d meshes from 2d text-to-image models. In *Proceedings of the IEEE/CVF International Conference on Computer Vision*, pages 7909–7920, 2023. 2
- [18] Dong Huo, Zixin Guo, Xinxin Zuo, Zhihao Shi, Juwei Lu, Peng Dai, Songcen Xu, Li Cheng, and Yee-Hong Yang. Texgen: Text-guided 3d texture generation with multi-view sampling and resampling. *arXiv preprint arXiv:2408.01291*, 2024. 2
- [19] Bernhard Kerbl, Georgios Kopanas, Thomas Leimkühler, and George Drettakis. 3d gaussian splatting for real-time radiance field rendering. *ACM Trans. Graph.*, 42(4):139–1, 2023. 2
- [20] Ruoshi Liu, Rundi Wu, Basile Van Hoorick, Pavel Tokmakov, Sergey Zakharov, and Carl Vondrick. Zero-1-to-3: Zero-shot one image to 3d object. In *Proceedings of the IEEE/CVF international conference on computer vision*, pages 9298–9309, 2023. 4
- [21] Yuxin Liu, Minshan Xie, Hanyuan Liu, and Tien-Tsin Wong. Text-guided texturing by synchronized multi-view diffusion. *arXiv preprint arXiv:2311.12891*, 2023. 2, 4
- [22] Andreas Lugmayr, Martin Danelljan, Andres Romero, Fisher Yu, Radu Timofte, and Luc Van Gool. Repaint: Inpainting using denoising diffusion probabilistic models. In *Proceedings of the IEEE/CVF conference on computer vision and pattern recognition*, pages 11461–11471, 2022. 5
- [23] Weijia Mao, Yan-Pei Cao, Jia-Wei Liu, Zhongcong Xu, and Mike Zheng Shou. Showroom3d: Text to high-quality 3d room generation using 3d priors. *arXiv preprint arXiv:2312.13324*, 2023. 2
- [24] Gal Metzger, Elad Richardson, Or Patashnik, Raja Giryes, and Daniel Cohen-Or. Latent-nerf for shape-guided generation of 3d shapes and textures. In *Proceedings of the IEEE/CVF Conference on Computer Vision and Pattern Recognition*, pages 12663–12673, 2023. 1, 2
- [25] Ben Mildenhall, Pratul P. Srinivasan, Matthew Tancik, Jonathan T. Barron, Ravi Ramamoorthi, and Ren Ng. Nerf:

- Representing scenes as neural radiance fields for view synthesis. In *ECCV*, 2020. 2
- [26] Chong Mou, Xintao Wang, Liangbin Xie, Yanze Wu, Jian Zhang, Zhongang Qi, and Ying Shan. T2i-adapter: Learning adapters to dig out more controllable ability for text-to-image diffusion models. In *Proceedings of the AAAI Conference on Artificial Intelligence*, pages 4296–4304, 2024. 2
- [27] Hao Ouyang, Kathryn Heal, Stephen Lombardi, and Tiancheng Sun. Text2immersion: Generative immersive scene with 3d gaussians. *arXiv preprint arXiv:2312.09242*, 2023. 2
- [28] Dustin Podell, Zion English, Kyle Lacey, Andreas Blattmann, Tim Dockhorn, Jonas Müller, Joe Penna, and Robin Rombach. Sdxl: Improving latent diffusion models for high-resolution image synthesis. *arXiv preprint arXiv:2307.01952*, 2023. 1, 2, 4, 6
- [29] Ben Poole, Ajay Jain, Jonathan T Barron, and Ben Mildenhall. Dreamfusion: Text-to-3d using 2d diffusion. *arXiv preprint arXiv:2209.14988*, 2022. 2
- [30] Aditya Ramesh, Mikhail Pavlov, Gabriel Goh, Scott Gray, Chelsea Voss, Alec Radford, Mark Chen, and Ilya Sutskever. Zero-shot text-to-image generation. In *International Conference on Machine Learning*, pages 8821–8831. PMLR, 2021. 1
- [31] Nikhila Ravi, Jeremy Reizenstein, David Novotny, Taylor Gordon, Wan-Yen Lo, Justin Johnson, and Georgia Gkioxari. Accelerating 3d deep learning with pytorch3d. *arXiv:2007.08501*, 2020. 7
- [32] Elad Richardson, Gal Metzer, Yuval Alaluf, Raja Giryes, and Daniel Cohen-Or. Texture: Text-guided texturing of 3d shapes. In *ACM SIGGRAPH 2023 conference proceedings*, pages 1–11, 2023. 1, 2, 3, 4
- [33] Robin Rombach, Andreas Blattmann, Dominik Lorenz, Patrick Esser, and Björn Ommer. High-resolution image synthesis with latent diffusion models. In *Proceedings of the IEEE/CVF Conference on Computer Vision and Pattern Recognition (CVPR)*, pages 10684–10695, 2022. 1, 2
- [34] Chitwan Saharia, William Chan, Saurabh Saxena, Lala Li, Jay Whang, Emily L Denton, Kamyar Ghasemipour, Raphael Gontijo Lopes, Burcu Karagol Ayan, Tim Salimans, et al. Photorealistic text-to-image diffusion models with deep language understanding. *Advances in Neural Information Processing Systems*, 35:36479–36494, 2022. 1, 2
- [35] Christoph Schuhmann, Richard Vencu, Romain Beaumont, Robert Kaczmarczyk, Clayton Mullis, Aarush Katta, Theo Coombes, Jenia Jitsev, and Aran Komatsuzaki. Laion-400m: Open dataset of clip-filtered 400 million image-text pairs. *arXiv preprint arXiv:2111.02114*, 2021. 7, 8
- [36] Ruoxi Shi, Hansheng Chen, Zhuoyang Zhang, Minghua Liu, Chao Xu, Xinyue Wei, Linghao Chen, Chong Zeng, and Hao Su. Zero123++: a single image to consistent multi-view diffusion base model. *arXiv preprint arXiv:2310.15110*, 2023. 4
- [37] Yichun Shi, Peng Wang, Jianglong Ye, Mai Long, Kejie Li, and Xiao Yang. Mvdream: Multi-view diffusion for 3d generation. *arXiv preprint arXiv:2308.16512*, 2023. 4
- [38] Jascha Sohl-Dickstein, Eric Weiss, Niru Maheswaranathan, and Surya Ganguli. Deep unsupervised learning using nonequilibrium thermodynamics. In *International conference on machine learning*, pages 2256–2265. PMLR, 2015. 3
- [39] Jiayang Tang, Ruijie Lu, Xiaokang Chen, Xiang Wen, Gang Zeng, and Ziwei Liu. Intex: Interactive text-to-texture synthesis via unified depth-aware inpainting. *arXiv preprint arXiv:2403.11878*, 2024. 2
- [40] Shitao Tang, Fuyang Zhang, Jiacheng Chen, Peng Wang, and Yasutaka Furukawa. Mvdifffusion: Enabling holistic multi-view image generation with correspondence-aware diffusion. *arXiv*, 2023. 4
- [41] Zhenyu Tang, Junwu Zhang, Xinhua Cheng, Wangbo Yu, Chaoran Feng, Yatian Pang, Bin Lin, and Li Yuan. Cycle3d: High-quality and consistent image-to-3d generation via generation-reconstruction cycle. *arXiv preprint arXiv:2407.19548*, 2024. 2
- [42] Haochen Wang, Xiaodan Du, Jiahao Li, Raymond A Yeh, and Greg Shakhnarovich. Score jacobian chaining: Lifting pretrained 2d diffusion models for 3d generation. In *Proceedings of the IEEE/CVF Conference on Computer Vision and Pattern Recognition*, pages 12619–12629, 2023.
- [43] Zhengyi Wang, Cheng Lu, Yikai Wang, Fan Bao, Chongxuan Li, Hang Su, and Jun Zhu. Prolificdreamer: High-fidelity and diverse text-to-3d generation with variational score distillation. *Advances in Neural Information Processing Systems*, 36, 2024. 2
- [44] Jinbo Xing, Menghan Xia, Yong Zhang, Haoxin Chen, Wangbo Yu, Hanyuan Liu, Gongye Liu, Xintao Wang, Ying Shan, and Tien-Tsin Wong. Dynamicrafter: Animating open-domain images with video diffusion priors. In *ECCV*, 2024. 2
- [45] Bangbang Yang, Wenqi Dong, Lin Ma, Wenbo Hu, Xiao Liu, Zhaopeng Cui, and Yuewen Ma. Dreamspace: Dreaming your room space with text-driven panoramic texture propagation. In *2024 IEEE Conference Virtual Reality and 3D User Interfaces (VR)*, pages 650–660. IEEE, 2024. 3
- [46] Jonathan Young. xatlas. In *github.com/jpcy/xatlas*, 2016. 7
- [47] Kim Youwang, Tae-Hyun Oh, and Gerard Pons-Moll. Paintit: Text-to-texture synthesis via deep convolutional texture map optimization and physically-based rendering. In *Proceedings of the IEEE/CVF Conference on Computer Vision and Pattern Recognition*, pages 4347–4356, 2024. 1, 2
- [48] Wangbo Yu, Li Yuan, Yan-Pei Cao, Xiangjun Gao, Xiaoyu Li, Wenbo Hu, Long Quan, Ying Shan, and Yonghong Tian. Hifi-123: Towards high-fidelity one image to 3d content generation. *arXiv preprint arXiv:2310.06744*, 2023. 2
- [49] Wangbo Yu, Jinbo Xing, Li Yuan, Wenbo Hu, Xiaoyu Li, Zhipeng Huang, Xiangjun Gao, Tien-Tsin Wong, Ying Shan, and Yonghong Tian. Viewcrafter: Taming video diffusion models for high-fidelity novel view synthesis. *arXiv preprint arXiv:2409.02048*, 2024. 2
- [50] Jingbo Zhang, Xiaoyu Li, Ziyu Wan, Can Wang, and Jing Liao. Text2nerf: Text-driven 3d scene generation with neural radiance fields. *IEEE Transactions on Visualization and Computer Graphics*, 2024. 2
- [51] Lvmin Zhang, Anyi Rao, and Maneesh Agrawala. Adding conditional control to text-to-image diffusion models. In

Proceedings of the IEEE/CVF International Conference on Computer Vision, pages 3836–3847, 2023. [1](#), [2](#), [4](#), [6](#)

- [52] Haiyang Zhou, Xinhua Cheng, Wangbo Yu, Yonghong Tian, and Li Yuan. Holodreamer: Holistic 3d panoramic world generation from text descriptions. *arXiv preprint arXiv:2407.15187*, 2024. [2](#)